

Preprocessing of SPECT Projection Data: Benefits and Pitfalls

A. Hans Vija, Amos Yahil, Eric G. Hawman, *Members IEEE*

Abstract—The Pixon¹ method, a statistically rigorous procedure for adaptive noise suppression that avoids the generation of spurious artifacts yet preserves all the statistically justifiable image features resident in the raw counts, is applied to nuclear studies. The present work focuses on the denoising of projection data at various count levels for subsequent SPECT iterative reconstructions, where each projection is denoised independently. The pitfall of applying such preprocessing to projection images is that tomographic information could be lost, resulting in the loss of weak or small sources. The goal is to investigate the benefits and pitfalls of noise suppression of projection data on the resulting reconstruction, with the ultimate goals to (i) increase sensitivity for detection of lesions of small size and/or of small activity-to-background ratio, (ii) reduce data acquisition time, and (iii) reduce patient dose. We use simulated and measured data and human observer studies, which are analyzed using quantitative measures. **Conclusion:** An accurate reconstruction at reduced counts using view-independent, noise-reduced projection images can result in significant gain in detectability based on simple SNR measures, but only minor improvements as tested with human observers. At the same time, conservative denoising of the projections results in the loss of small and weak sources, particularly cold lesions. Further analysis and clinical feedback may be warranted, yet it seems that such an approach contains serious pitfalls, likely outweighing the benefits.

I. INTRODUCTION

The unique Pixon method for the suppression of random noise in images, initially developed for astronomical applications [1–3], is adapted and applied to nuclear medical imaging. The method is a statistically rigorous procedure for noise suppression that avoids the generation of spurious artifacts yet preserves all the statistically justifiable image features resident in the raw counts. The method optimizes noise suppression by taking full advantage of the local information content of the image and avoiding global noise-suppression criteria [4–7], which may not be locally optimal. Pixon processing is therefore especially well suited to imag-

ing at low signal-to-noise ratio and is particularly attractive for applications in nuclear medicine [8–9]. The present work focuses on preprocessing projection data for subsequent SPECT iterative reconstructions, where each projection is preprocessed independently. The pitfall of applying such preprocessing to tomographic projection images is that tomographic information is lost, thereby eliminating weak sources or losing resolution. The goal is to investigate the benefits and pitfalls of noise suppression of SPECT projection data on the resulting reconstructions, with the ultimate goals to (i) increase sensitivity for detection of lesions of small size and/or of small activity-to-background ratio, (ii) reduce data acquisition time, and (iii) reduce patient dose. We use both simulated and measured phantom data at various count levels. The objects are cylindrical phantoms with sphere or rod inserts, reconstructed with Flash3D² (OSEM) with 3D collimator blur compensation, CT attenuation correction and scatter compensation.

II. METHODS

The key objective of the Pixon method is to generate an output image that is as smooth as possible yet statistically consistent with the raw counts, given the noise and image formation model. Here the noise model is Poisson noise and the image formation is projection imaging by a parallel-hole collimator. The method is a nonparametric, spatially adaptive smoothing algorithm, in which the width of the smoothing kernel at each image location is adjusted to the local image conditions [1–3,8]. Where the underlying image is uniform, or the signal-to-noise ratio is not high, it is possible to smooth over a wider span of pixels without loss of information; where the underlying image varies significantly relative to the noise, the smoothing kernel is restricted to fewer pixels to avoid loss of resolution. The local information content of the image, and only the local information content, determines the best smoothing scale.

As an example for the planar denoising ability, Fig.1 shows planar acquisitions of the rod phantom at varying counts processed with the Pixon method [9]. The remarkable abil-

Manuscript received Nov. 11, 2005.

A. Hans Vija (e-mail: hans.vija@siemens.com), Eric G. Hawman (e-mail: eric.hawman@siemens.com) are with Siemens Medical Solutions USA, Inc., Molecular Imaging, Hoffman Estates, IL 60195, USA.

Amos Yahil (e-mail: amos.yahil@pixon.com) is with Pixon, LLC, Stony Brook, NY 11790, USA.

¹ Pixon[®] is a registered trademark of Pixon LLC.

² Flash3D is the OSEM iterative reconstruction with collimator blur modeling in the transverse and axial directions of Siemens Medical Solutions USA, Inc., Molecular Imaging.

ity to extract the rod structure from the very noisy 100 kc image is clearly demonstrated.

Noiseless simulated projections are generated using a ray tracing method and from this 10 Poisson realizations at varying count levels [1.7, 2.9, 5*n, n=1...8. units: kc/view] are generated. This simulates the acquisition of Data Spectrum's Cylinder with the 6 spheres (0.5 – 16 ml) at a 5:1 concentration ratio in a 128x128 matrix with 4.8 mm pixels, and 60 views over a 180-degree arc at 25 cm. The data are then denoised with the Pixon method and reconstructed with Flash3D using perfect attenuation, scatter and collimator compensation. Here the Pixon method is only used to reduce noise, and not to compensate for the collimator blur, as this is taken into consideration in the reconstruction. Please note that in this study the term "preprocessing" is used to describe noise reduction of each view of the tomographic projection data as if these projections have no relationship to each other. The Pixon noise-reduction (smoothness) parameter dn [8] is deliberately set to the low value of 1.0, which minimizes loss of tomographic information while providing some denoising, and to 1.75, which corresponds to optimal planar processing of the data, resulting in a cumulative distribution function (CDF) consistent with maximal information extraction [9]. Real data are acquired on a Symbia TruePoint SPECT-CT using Data Spectrum's Cylinder loaded with ^{99m}Tc with the rod and sphere inserts (peak window center: 140keV with a width of 15%, 3.3 mm pixel, 128²-matrix, 25 cm rotation radius). The acquisitions are stopped on counts (250kc/view) and subsampled to obtain any count level between 0 and 250 kc/view. A corresponding attenuation map is derived from a CT scan for attenuation correction.

We investigate the effects of noise suppression on the reconstruction. One of the quantitative measures is an SNR measure, the detectability index DI, defined as the difference between the average counts per pixel in the spheres (S) and the background (B) ROI, normalized by the noise in the background (N): $DI = (\langle S \rangle - \langle B \rangle) / \langle N \rangle$, where the angular brackets indicate averaging over pixels in the ROI and all realizations. DI increases if the noise in the image is reduced and signal preserved. Besides DI and a quantitative resolution analysis, we use a human observer detection task study to assess the performance differences between Flash3D reconstructions using various preprocessed and unprocessed projections. For this, 10 readers are asked to identify the presence of a sphere of unknown size and location. They are, however, instructed that the image contains either one sphere or no source. Each reader has a set of 180 reconstructed slices, half of which are placebo (from slices that do not intersect any sphere). The 90 cases correspond to 10 noise levels, 3 sphere volumes (0.5 ml, 1 ml, or 2 ml), and 3 denoising parameters (dn=0, i.e., no preprocessing, 1.0, or 1.75). All cases are reconstructed with Flash3D and subsequent 3D Gaussian postsmoothing with a FWHM of 2

pixels. The reader is simply asked whether or not he detects a sphere anywhere in the image, and the response is recorded automatically together with the decision time. The reader is allowed to change the windowing parameters (upper and lower cutoffs and the gamma parameter of the gray scale images). This freedom is chosen to simulate clinical reality.

III. RESULTS

The results are shown in Fig. 2–10; we skip a detailed description of the results due to space constraints.

IV. DISCUSSION

This project attempts to investigate the benefits and pitfalls of denoising or smoothing of tomographic projection data. It is important to note that each projection view is processed independently, as if the other views do not exist. The pitfall is that any smoothing method, which has to decide, what is signal and what is noise based on some criteria, may consider a feature in any projection as noise, while a reconstruction of the entire projection set would reveal it to be signal. This causes degradation of the tomographic data, and the result is loss of resolution. The detection of hot lesions may be improved by the suppression of background noise, albeit with possible loss of resolution as to detail, but the detection of cold lesion suffers because of the preprocessing. In this work we look carefully at simulation data at different noise levels of a hot-spheres phantom, and apply the statistically and spatially adaptive, mathematically rigorous and conservative smoothing Pixon method to the projection data. The optimal smoothing parameter dn is chosen so that the residuals are consistent with white Poisson noise [3,9]. At this operating point the best possible information extraction of a projection has occurred and this is used in the subsequent reconstruction. A planar "suboptimal" denoising of dn=1.0 is also chosen to reflect the knowledge that the projection data really are part of a tomographic data set, and thus optimal planar denoising may not be optimal for the reconstruction.

The DI shows improvement when the total counts are increased (Fig. 1–2), when the volume of the sphere increases (Fig. 3) and also when the denoising is increased by increasing the denoising parameter dn. Using human readers to detect the 3 smallest spheres (0.5 ml, 1 ml and 2 ml) the detection ability between the methods is not as large as the DI would indicate, as Fig. 4–5 show. The false-positive fraction (FPF) shows a constant value ~20% for all count levels and all preprocessing methods, indicating that the placebos are identified as such rather well. This may be due to the study design; a better way would have been to ask the reader to identify the spheres without a priori knowledge of the maximum number of spheres in the image. The lack of dependence of the FPF on the parameters of the experiment

means that the ROC study should be revised. In future studies we also plan to vary the concentration ratio of the spheres, with the expectation that there will be more significant false positives when it is low.

When the method is applied to patient or phantom data, however, the pitfalls of preprocessing become very clear. The bone study in Fig. 6 shows the loss of resolution as seen by the 2 lesions in the transverse slice as the denoising is increased. The pitfalls are shown more dramatically in the cold section of the Hot-Cold-Rod phantom (Fig. 7–9); the cold rods even disappear in Fig. 9, in which the optimal planar denoising ($dn=1.75$) is used. This is, after all, not surprising. Cold lesions probe a very difficult statistical regime: few counts in an ROI surrounded by higher counts and thus better statistics. Based on statistical analysis and a set confidence level (denoise parameter) a count depression could easily be justified for smoothing if each planar view is analyzed individually. Hot lesions, on the other hand, fair better, and the resolution loss is not as dramatic, although present (Fig. 10). In fact, Flash3D reconstructs the 25% and 50% count-reduced data rather well, and the detectability or resolution is hardly affected. For comparison, we also show the data reconstructed by filtered back projection (FBP) at 100% of the counts without any preprocessing.

V. CONCLUSIONS

Given the minor improvement of detectability and major drawback of reduced resolution, with potential loss of clinically relevant information, one can only warn against using any type of denoising of projection data prior to a nonlinear tomographic reconstruction.³ Cold lesions are particularly prone to loss of information by preprocessing.

Count reduction due to the reduction of acquisition time and/or dose increases noise in the data, and this has to be handled properly. In this study even the most conservative and statistically rigorous denoising method does not mitigate the risk of resolution loss in the reconstruction. One is better off using iterative reconstruction which accurately models the imaging physics, such as an OSEM with 3D beam modeling (e.g. Flash3D) instead of denoising the projections before reconstruction.

VI. REFERENCES

[1] Piña RK, Puetter RC, “Bayesian image reconstruction: The Pixon and optimal image modeling” *Publ Astron Soc Pac*, 1993, 105, 630–637
 [2] Puetter RC, Yahil, A, “The Pixon method of image reconstruction”, in: *Astronomical Data Analysis Software and Systems VIII*. Mehringer DM, Plante RL, Roberts DA, Eds. San Francisco: Astronomical Society of the Pacific Conference Series, 1998, 172, 307–316

[3] Puetter RC, Gosnell, GR, Yahil, A, “Digital image reconstruction: deblurring and denoising”, *Annu. Rev. Astron. Astrophys.*, 2005, 43, 139–194
 [4] Gwiazdowska BA, Skrzypczak ET, Tolwinski JR, “The evaluation of noise reduction and resolution degradation in scintigraphic images due to smoothing procedures” *Nuklearmedizin*, 1982, 21, 126–129
 [5] Kunni CC, Hasegawa BH, Hende WR, “Noise reduction in nuclear medicine images” *J. Nucl. Med.*, 1983, 24, 532–534
 [6] Riddell C, Carson RE, Carrasquillo JA, et al, “Noise Reduction in oncology FDG PET images by iterative reconstruction: a quantitative assessment” *J. Nucl. Med.*, 2001, 42, 1316–1323
 [7] Hannequin P, Mas J, “Statistical and heuristic noise extraction (SHINE): a new method for processing Poisson noise in scintigraphic images” *Phys. Med. Biol.*, 2002, 47, 4329–4344
 [8] Wesolowski CA, Yahil A, Puetter RC, Babyn PS, Gilday DL, Khan MZ, “Improved lesion detection from spatially adaptive, minimally complex, Pixon® reconstruction of planar scintigraphic images”, 2005, *Comput. Med. Imaging Graph.*, 29, 65–81
 [9] Vija AH, Gosnell TR, Yahil A, Hawman EG, Engdahl JC, “Statistically based, spatially adaptive noise reduction of planar nuclear studies”, 2005, *Proc. SPIE 5747*, 634–645

VII. ACKNOWLEDGMENT

The authors would like to thank the observer study participants at Siemens Molecular Imaging.

VIII. FIGURES

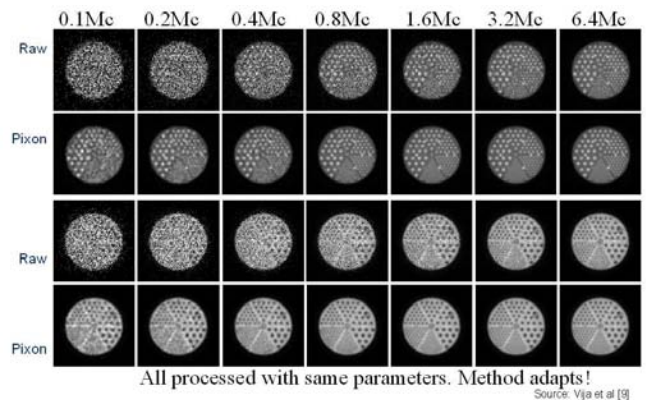


Fig. 1: Raw and Pixon-processed planar images of hot and cold sections of the rod phantom acquired to range of total counts between 100 kc and 6400 kc. Once the denoising parameter dn is adjusted to 1.75 according to the CDF result no further change in the processing parameters is needed [9].

³ Filtering and reconstruction commute, of course, if the process is strictly linear, in which case they can be performed in any order.

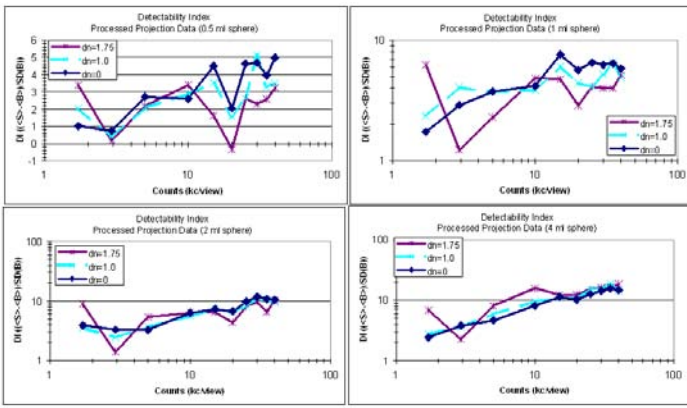


Fig. 2: Detectability index for the 0.5,1,2,4 ml spheres at varying counts and preprocessing parameters.

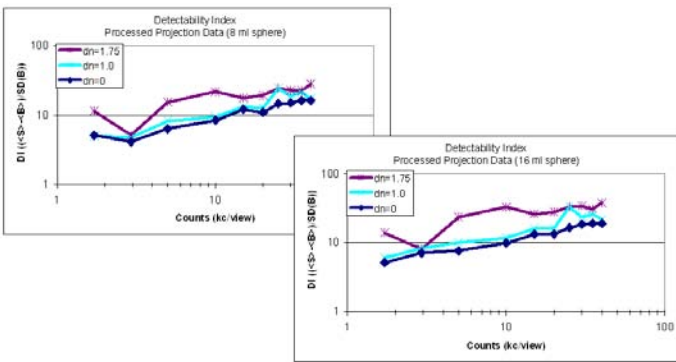


Fig. 3: Detectability index for the 8, and 16 ml spheres at the varying counts and preprocessing parameters.

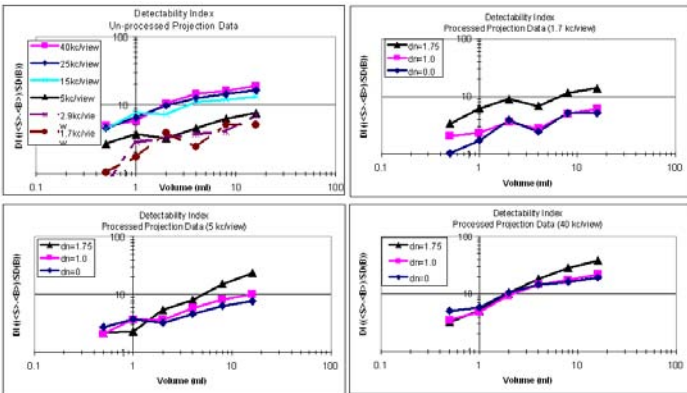


Fig. 4: Detectability index for all spheres at the various counts with and without preprocessing.

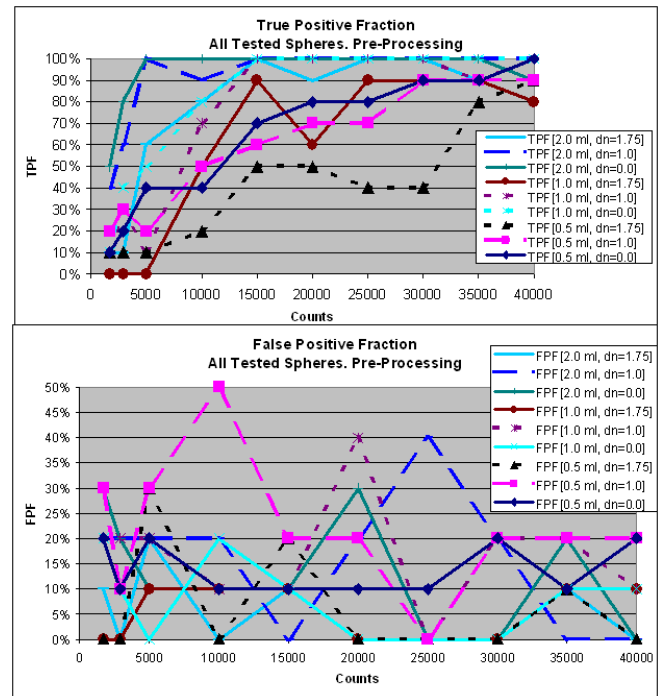


Fig. 5: True and False Positive Fraction (TPF, FPF) for varying spheres at the various counts and preprocessing method. Note1: TPF essentially increases as counts increase. Note2: FPF is essentially constant.

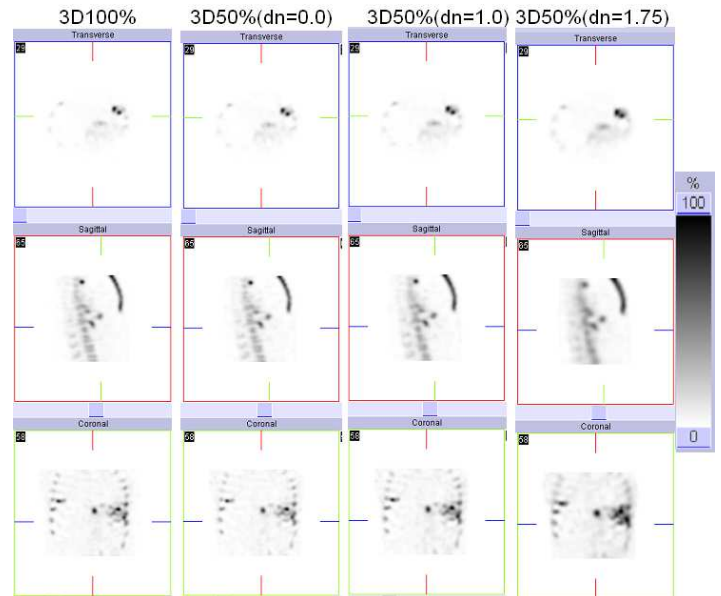


Fig. 6: Resolution loss example. Bone study at 100% and 50% subsampled counts without and with preprocessing at dn=1.0, and dn=1.75. Flash3D at 50% shows better resolution than denoising of projection data.

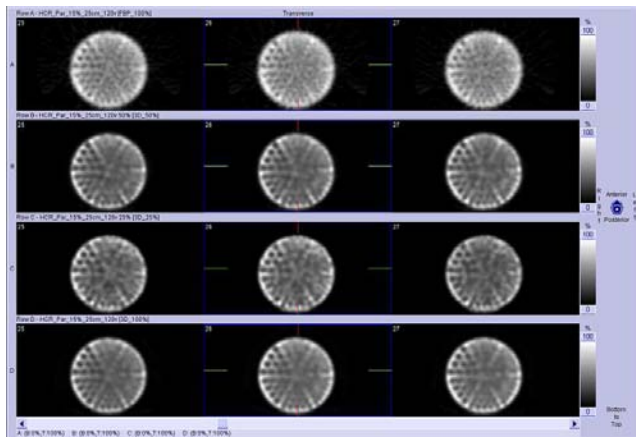


Fig. 7: No denoising prior reconstruction using FBP and Flash3D (OSEM with 3 beam modeling). Row1: FBP (100%), Row2-4: Flash3D at 50%, 25%, 100% counts

(100%) no denoising, Row2-4: Flash3D at 50%, 25%, 100% counts and $dn=1.75$. Cold Rod Resolution severely affected.

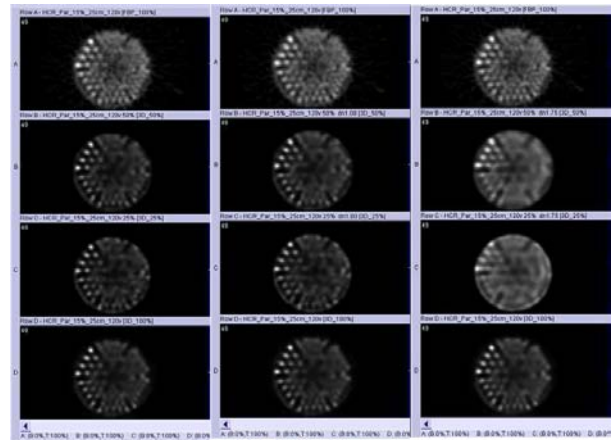


Fig. 10: Planar “optimal” denoising prior reconstruction using FBP and Flash3D (OSEM with 3 beam modeling). Row1: FBP (100%) no denoising, Row2-4: Flash3D at 50%, 25%, 100% counts and $dn=1.75$. Hot Rod resolution only minorly affected.

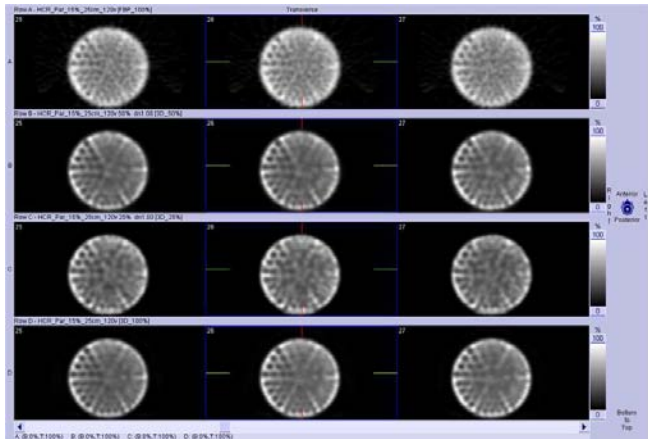


Fig. 8: Slight denoising prior reconstruction using FBP and Flash3D (OSEM with 3 beam modeling). Row1: FBP (100%) no denoising, Row2-4: Flash3D at 50%, 25%, 100% counts and $dn=1.0$. Cold Rod resolution affected.

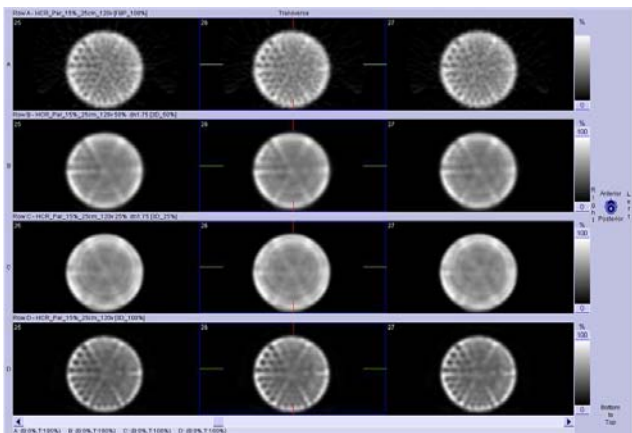


Fig. 9: Planar “optimal” denoising prior reconstruction using FBP and Flash3D (OSEM with 3 beam modeling). Row1: FBP